RSC Advances

PAPER

View Article Online
View Journal | View Issue

Cite this: *RSC Adv.*, 2018, **8**, 13040

Anti-inflammatory butenolide derivatives from the coral-derived fungus *Aspergillus terreus* and structure revisions of aspernolides D and G, butyrolactone VI and 4′,8″-diacetoxy butyrolactone VI†

Mengting Liu,‡[a] Qun Zhou,‡[a] Jianping Wang,‡[a] Junjun Liu,[a] Changxing Qi,[a] Yongji Lai,[b] Hucheng Zhu,[a] Yongbo Xue,[a] Zhengxi Hu*[a] and Yonghui Zhang*[a]

Chemical investigation of the coral-derived fungus *Aspergillus terreus* led to the discovery of ten butenolide derivatives (**1–10**), including four new ones (**1–4**). The new structures were characterized on the basis of comprehensive spectroscopic analysis, including 1D and 2D NMR and HRESIMS data. Compounds **1** and **2** were a pair of rare C-8″ epimers with vicinal diol motifs. The absolute configurations of **1–4** were determined *via* $[Mo_2(AcO)_4]$ induced circular dichroism (ICD) spectra and comparison of their experimental ECD spectra. Importantly, the structures of reported aspernolides D and G, butyrolactone VI and 4′,8″-diacetoxy butyrolactone VI have been correspondingly revised *via* a combined strategy of experimental validations, ^{13}C NMR predictions by ACD/Labs software, and ^{13}C NMR calculations. Herein we provide valuable referenced ^{13}C NMR data (C-7″, C-8″, and C-9″) for the structure elucidations of butenolide derivatives with 1-(2-hydroxyphenyl)-3-methylbutane-2,3-diol, 2-(2,3-dihydrobenzofuran-2-yl)propan-2-ol, or 2,2-dimethylchroman-3-ol motifs. Additionally, all the isolates (**1–10**) were assessed for anti-inflammatory activity by measuring the amount of NO production in lipopolysaccharide (LPS)-induced RAW 264.7 mouse macrophages, and compound **10** showed an even stronger inhibitory effect than the postive control indomethacin, presenting it as a promising lead compound for the development of new anti-inflammatory agents.

Received 2nd March 2018
Accepted 2nd April 2018

DOI: 10.1039/c8ra01840e

rsc.li/rsc-advances

Introduction

Microorganisms have been regarded as an under-explored source of structurally interesting and bioactive natural products with the potential to provide attractive lead compounds for drug discovery.[1] As one of the most useful fungi, the *Aspergillus* genus was found to have powerful clusters to biosynthesize plenty of complex secondary metabolites,[2] including lignans, alkaloids, terpenes, polyketides, peptides, *etc.*, showing intriguing pharmaceutical activities, upon which some groundbreaking research has been finished by our research group. For example, *Aspergillus flavipes* produces several bioactive merocytochalasans (anti-tumor agents), namely asperchalasine A,[3] epicochalasines A and B,[4] asperflavipine A,[5] and aspergilasines A–D,[6] which were characterized by architecturally complex polycyclic rings and multiple chiral centers; *Aspergillus terreus* produces two unprecedented meroterpenoids, namely asperterpenes A and B,[7] showing potent BACE1 inhibitory activities for Alzheimer's disease treatment; *Aspergillus* sp. TJ23 produces

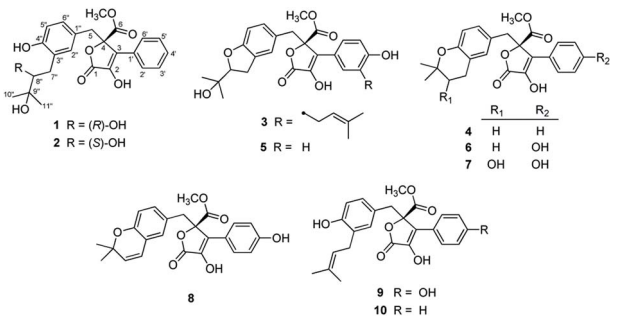

Fig. 1 Chemical structures of compounds **1–10**.

[a]*Hubei Key Laboratory of Natural Medicinal Chemistry and Resource Evaluation, School of Pharmacy, Tongji Medical College, Huazhong University of Science and Technology, Wuhan 430030, Hubei Province, People's Republic of China. E-mail: zhangyh@mails.tjmu.edu.cn; hzx616@126.com; Fax: +86-27-83692762; Tel: +86-27-83692892*

[b]*Department of Pharmacy, The Central Hospital of Wuhan, Wuhan 430014, Hubei Province, People's Republic of China*

† Electronic supplementary information (ESI) available: The 1D and 2D NMR, HRESIMS, IR, and UV spectra of compounds **1–4**. See DOI: 10.1039/c8ra01840e

‡ These authors contributed equally to this work.

a bridged spirocyclic meroterpenoid, namely spiroaspertrione A,[8] which was found to be a PBP2a inhibitor and act as a potent potentiator of oxacillin against methicillin-resistant *Staphylococcus aureus*. Inspired by these structurally unexpected natural products with tempting pharmacological activities from the *Aspergillus* genus, we are devoted to the investigation of *Aspergillus* species from different origins for chemical and pharmacological diversity.

In our efforts to explore bioactive natural products from marine-derived fungi,[9] we performed a chemical investigation on the fermented rice substrate of a coral-derived fungus *Aspergillus terreus*, resulting in the isolation of ten butenolide derivatives (**1–10**), including four new ones (**1–4**), wherein **1** and **2** were a pair of rare C-8″ epimers with vicinal diol motifs. Importantly, the NMR data of **5** and **7** were closely similar to those of reported aspernolide D[10] and butyrolactone VI,[11] which inspired us to perform the structure reassignments of reported aspernolides D and G, butyrolactone VI and 4′,8″-diacetoxy butyrolactone VI, as assisted by a combined strategy of experimental validations, ^{13}C NMR predictions by ACD/Labs software, and ^{13}C NMR calculations. Herein, we report the isolation, structure elucidation, structure reassignments, and anti-inflammatory activity of these butenolide derivatives (Fig. 1).

Table 1 ^{1}H and ^{13}C NMR data for compounds **1–4** (δ in ppm and J in Hz)

	1		**2**		**3**		**4**	
No.	$\delta_H{}^{a,b,d}$	$\delta_C{}^{c,d}$	$\delta_H{}^{a,b,d}$	$\delta_C{}^{c,d}$	$\delta_H{}^{a,b,e}$	$\delta_C{}^{c,e}$	$\delta_H{}^{a,b,e}$	$\delta_C{}^{c,e}$
1	—	170.0 C	—	170.1 C	—	171.8 C	—	170.0 C
2	—	140.3 C	—	140.4 C	—	140.4 C	—	142.1 C
3	—	127.8 C	—	127.5 C	—	129.5 C	—	128.6 C
4	—	86.2 C	—	86.2 C	—	87.0 C	—	86.9 C
5	3.50 m	38.7 CH_2	3.51 d (4.2)	38.6 CH_2	3.44 d (9.1)	39.7 CH_2	3.42 d (1.6)	39.4 CH_2
6	—	170.0 C	—	170.1 C	—	171.8 C	—	171.4 C
6-OMe	3.76 s	53.8 CH_3	3.78 s	53.8 CH_3	3.77 s	53.8 CH_3	3.76 s	53.9 CH_3
1′	—	130.2 C	—	130.4 C	—	125.2 C	—	131.9 C
2′	7.66 d (7.7)	127.7 CH	7.71 d (7.8)	127.5 CH	6.45 d (2.1)	132.5 CH	7.64 d (7.4)	128.6 CH
3′	7.40 dd (7.3, 7.7)	129.1 CH	7.42 dd (7.1, 7.8)	129.2 CH	—	128.4 C	7.43 dd (7.3, 7.4)	129.8 CH
4′	7.35 dd (7.3, 7.3)	129.2 CH	7.33 dd (7.1, 7.1)	129.1 CH	—	155.1 C	7.35 dd (7.3, 7.3)	129.7 CH
5′	7.40 dd (7.3, 7.7)	129.1 CH	7.42 dd (7.1, 7.8)	129.2 CH	6.48 d (8.1)	115.1 CH	7.43 dd (7.3, 7.4)	129.8 CH
6′	7.66 d (7.7)	127.7 CH	7.71 d (7.8)	127.5 CH	6.53 dd (2.1, 8.1)	129.8 CH	7.64 d (7.4)	128.6 CH
7′	—	—	—	—	3.08 br d (7.4)	28.8 CH_2	—	—
8′	—	—	—	—	5.09 m	123.8 CH	—	—
9′	—	—	—	—	—	132.8 C	—	—
10′	—	—	—	—	1.67 s	26.0 CH_3	—	—
11′	—	—	—	—	1.59 s	17.8 CH_3	—	—
1″	—	124.9 C	—	124.7 C	—	124.7 C	—	125.4 C
2″	6.70 s	133.1 CH	6.35 s	133.2 CH	7.68 s	125.6 CH	6.41 d (2.1)	132.6 CH
3″	—	126.2 C	—	125.6 C	—	129.5 C	—	121.4 C
4″	—	154.5 C	—	154.5 C	—	161.6 C	—	154.3 C
5″	6.52 d (8.1)	116.5 CH	6.62 d (8.2)	116.5 CH	6.83 d (8.5)	110.1 CH	6.38 d (8.3)	117.4 CH
6″	6.29 d (8.1)	130.1 CH	6.64 d (8.2)	130.7 CH	7.43 d (8.5)	128.7 CH	6.45 dd (2.1, 8.3)	130.2 CH
7″	2.43 br d (14.0); 2.69 dd (10.2, 14.0)	33.7 CH_2	2.33 br d (14.0); 2.61 dd (10.2, 14.0)	33.9 CH_2	3.23 m	31.4 CH_2	2.51 m	23.2 CH_2
8″	3.48 m	81.2 CH	3.43 m	80.9 CH	4.66 dd (8.3, 9.5)	91.0 CH	1.67 t (6.8)	33.7 CH_2
9″	—	74.0 C	—	73.9 C	—	72.5 C	—	75.1 C
10″	1.14 s	22.5 CH_3	1.14 s	23.0 CH_3	1.28 s	25.1 CH_3	1.20 s	27.0 CH_3
11″	1.21 s	26.2 CH_3	1.19 s	26.3 CH_3	1.25 s	25.4 CH_3	1.20 s	27.1 CH_3

[a] Recorded at 400 MHz. [b] "m" means overlapped or multiplet with other signals. [c] Recorded at 100 MHz. [d] Recorded in $CDCl_3$. [e] Recorded in methanol-d_4.

Results and discussion

Compounds **1** and **2**, both obtained as white, amorphous powders, were identified to have the same molecular formula $C_{24}H_{26}O_8$, according to their HRESIMS and ^{13}C NMR data, indicative of twelve indices of hydrogen deficiency. The close resemblances of 1D and 2D NMR data (Table 1) of **1** and **2** indicated that both compounds were a pair of epimers. The IR spectrum of **1** showed broad and intense absorption bands for hydroxy (3433 cm^{-1}), ester/lactone carbonyl (1743 cm^{-1}) and aromatic rings (1617, 1501, 1438 cm^{-1}). In the ^1H NMR data of **1**, a 1,2,4-trisubstituted benzene motif was observed based on the ABX system for three aromatic protons (δ_H 6.70, s, H-2″; 6.52, d, J = 8.1 Hz, H-5″; 6.29, d, J = 8.1 Hz, H-6″). Additionally, the 1D NMR data also showed the signals of δ_H 7.66 (d, J = 7.7 Hz, H-2′, 6′)/δ_C 127.7 (C-2′, 6′), δ_H 7.40 (dd, J = 7.3, 7.7 Hz, H-3′, 5′)/δ_C 129.1 (C-3′, 5′), and δ_H 7.35 (dd, J = 7.3, 7.3 Hz, H-4′)/δ_C 129.2 (C-4′), indicating the presence of a mono-substituted benzene motif. These characteristic data suggested that compound **1** was a butenolide derivative.

Detailed analysis of the 1D and 2D NMR data of **1** implied that its structural features were closely related to those of the known compound versicolactone B (**10**),[12] whose absolute structure was confirmed by single-crystal X-ray diffraction analysis, with the only difference that a $\Delta^{8'',9''}$ double bond in **10** was replaced by an oxygenated methine carbon (δ_C 81.2, C-8″) and an oxygenated tertiary carbon (δ_C 74.0, C-9″) in **1**, as supported *via* the molecular formula $C_{24}H_{26}O_8$ required by its HRESIMS data and the HMBC correlations from H_3-10″ to C-8″ and C-9″. The gross structures of **1** and **2** were further defined as shown *via* 2D NMR analysis, including ^1H–^1H COSY and HMBC spectral data (Fig. 2).

To determine the absolute configurations, the experimental ECD spectra of compounds **1** and **2** were measured in MeOH (Fig. 3), which were identical to that of versicolactone B,[12] showing positive Cotton effects at approximately 203 and 307 nm and a negative Cotton effect at approximately 230 nm that were ascribed to the conjugated functionality of an α,β-unsaturated carboxylic ester motif linked to a benzene group. Thus, the C-4 in **1** and **2** were both defined to be *R*-configurations. Accordingly, compounds **1** and **2** should be a pair of C-8″ epimers.

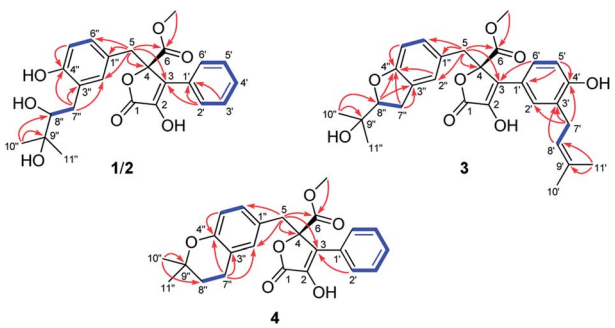

Fig. 2 Selected ^1H–^1H COSY (blue lines) and HMBC (red arrows) correlations of compounds **1**–**4**.

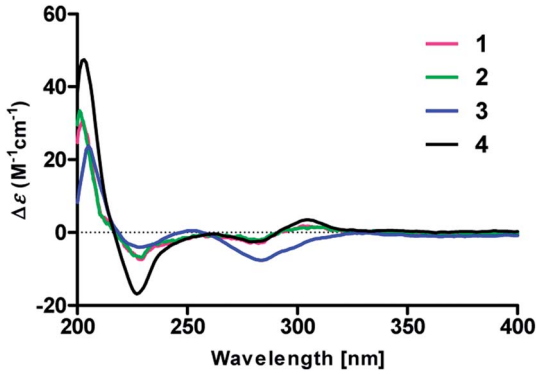

Fig. 3 Experimental ECD spectra of compounds **1**–**4** in MeOH.

The absolute configurations of 8″,9″-diol motifs in **1** and **2** were determined on the basic of *in situ* dimolybdenum CD method.[13] Compound **1** was mixed with $Mo_2(AcO)_4$ in DMSO to provide a metal complex, which showed a negative Cotton effect at approximately 305 nm (Fig. 4), permitting assignment of the 8″*R*-configuration for **1**, according to the empirical helicity rule relating the Cotton effect sign of the diagnostic O–C–C–O moiety.[13] Just using the same method like **1**, compound **2** showed a positive Cotton effect at approximately 305 nm (Fig. 4), thus suggesting the 8″*S*-configuration for **2**.[14] Therefore, the absolute structures of **1** and **2** were defined and named 8″*R*,9″-diol versicolactone B and 8″*S*,9″-diol versicolactone B, respectively.

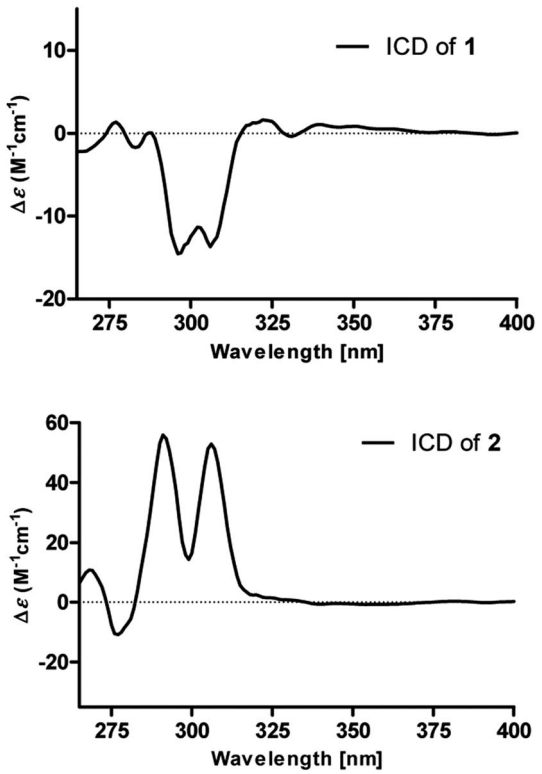

Fig. 4 $[Mo_2(OAc)_4]$ induced ICD spectra of **1** and **2** in DMSO.

Table 2 Comparison of chemical shifts of **1**, **5**, and **7** at C-7″, C-8″, and C-9″, respectively, *via* experimental validations, ^{13}C NMR predictions by ACD/Labs software, and ^{13}C NMR calculations (δ in ppm, in $CDCl_3$)

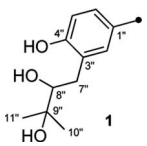

1

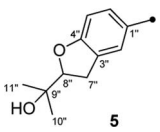

5

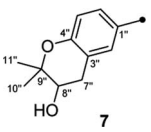

7

Compd no.	1-(2-Hydroxyphenyl)-3-methylbutane-2, 3-diol motif	2-(2,3-Dihydrobenzofuran-2-yl) propan-2-ol motif	2,2-Dimethylchroman-3-ol motif
Exptl chemical shifts			
7″	33.7	31.4	32.0
8″	81.2	90.4	70.4
9″	74.0	72.5	78.0
C + H NMR predictors and DB in ACD/Labs			
7″	32.0	30.1	30.8
8″	79.1	88.8	69.9
9″	73.5	71.9	77.5
Calcd chemical shifts			
7″	32.2	29.9	31.8
8″	76.0	85.3	67.1
9″	70.3	70.0	76.1

Compound **3** was obtained as a white, amorphous powder. The HRESIMS data showed a sodium adduct ion at *m*/*z* 531.1986 $[M + Na]^+$ (calcd for $C_{29}H_{32}O_8Na$, 531.1995), indicating a molecular formula of $C_{29}H_{32}O_8$. A direct comparison of its 1D NMR data (Table 1) with those of **5** indicated that a 1,4-disubstituted benzene motif in **5** was replaced by a 1,2,4-trisubstituted benzene group in **3** with an isopentene group positioned at C-3′, as supported by the ^{1}H–^{1}H COSY correlation of H_2-7′ and H-8′ and HMBC correlations from H_3-10′ and H_3-11′ to C-8′ and C-9′ and from H_2-7′ and H-8′ to C-3′ (δ_C 128.4) (Fig. 2). Moreover, the experimental ECD spectrum of **3** was related to those of **1** and **2** (Fig. 3), suggesting a 4*R*-configuration for **3**. Hence, the structure of **3** was defined and named 3′-isoamylene butyrolactone IV.

Compound **4**, also purified as a white, amorphous powder, was assigned the molecular formula $C_{24}H_{24}O_6$ based on HRESIMS data at *m*/*z* 431.1464 $[M + Na]^+$ (calcd for $C_{24}H_{24}O_6Na$, 431.1471). The ^{1}H and ^{13}C NMR data of **4** (Table 1) were similar to those of **6**, with the only difference being that a 1,4-disubstituted benzene motif in **6** was replaced by a mono-substituted benzene group linked to C-3 in **4**, as supported *via* the ^{1}H–^{1}H COSY correlations of H-2′/H-3′/H-4′/H-5′/H-6′ and HMBC correlation from H-2′ to C-3 (Fig. 2). Furthermore, the experimental ECD spectrum (Fig. 3) of **4** coincided well with those of **1** and **2**, suggesting that a 4*R*-configuration should also exist for **4**. Hence, the absolute structure of **4** was defined and named 4′-dehydroxy aspernolide A.

The six known butenolide derivatives were identified as butyrolactone IV (**5**),[15] aspernolide A (**6**),[16] butyrolactone V (**7**),[17] aspernolide E (**8**),[18] butyrolactone I (**9**),[12] and versicolactone B (**10**)[12] by comparison of their spectroscopic data with those reported in the literature.

On reviewing the literature, the pivotal ^{13}C NMR data for aspernolide D[10] [δ_C 30.5 (CH_2, C-7″) 89.1 (CH, C-8″), and 72.4 (C, C-9″)] and butyrolactone VI[11] [δ_C 31.0 (CH_2, C-7″) 69.6 (CH, C-8″), and 77.2 (C, C-9″)] showed close resemblances to those of compounds **5** and **7** (Table 2), respectively, which inspired us to investigate the regular ^{13}C NMR data of C-7″, C-8″, and C-9″ in the 1-(2-hydroxyphenyl)-3-methylbutane-2,3-diol, 2-(2,3-dihydrobenzofuran-2-yl)propan-2-ol, and 2,2-dimethylchroman-3-ol motifs for the butenolide derivatives. Take **1**, **5**, and **7** for examples (Table 2), their chemical shifts at C-7″ showed no obviously diagnostic differences; however, the chemical shifts at C-8″ and C-9″ showed apparent differences [δ_C 81.2 (C-8″) and 74.0 (C-9″) for **1**; δ_C 90.4 (C-8″) and 72.5 (C-9″) for **5**; δ_C 70.4 (C-8″) and 78.0 (C-9″) for **7**], corresponding to the predicted ^{13}C NMR data *via* "C + H NMR Predictor and DB" within the ACD/Labs software suite, which was regarded as a powerful and useful tool to predict the chemical shifts of a given input structure and resolve constitutional structure revisions.[19] The above-mentioned results indicated that aspernolide D and butyrolactone VI should be revised to **5** and **7** (Fig. 5), respectively, as supported by the calculations of ^{13}C NMR chemical shifts with two sets of R^2 values: 0.9946 for aspernolide D and 0.9986 for **5** (Fig. 6); 0.9929 for butyrolactone VI and 0.9983 for **7** (Fig. 7). Accordingly, the acetylated product of butyrolactone VI [δ_C 28.1 (CH_2, C-7″) 70.9 (CH, C-8″), and 75.1 (C, C-9″)],[11] named 4′,8″-diacetoxy butyrolactone VI, was also revised to **11** (Fig. 5) with an identical 2,2-dimethylchroman-3-ol motif. In addition, the ^{13}C NMR data [δ_C 31.4 (CH_2, C-7″) 68.4 (CH, C-8″), and 77.4 (C, C-9″)] of aspernolide G[20] were very consistent with those of **7** [δ_C 32.0 (CH_2, C-7″) 70.4 (CH, C-8″), and 78.0 (C, C-9″)] (Table 2), indicating that aspernolide G should be revised to **12** (Fig. 5). Remarkably, our current work

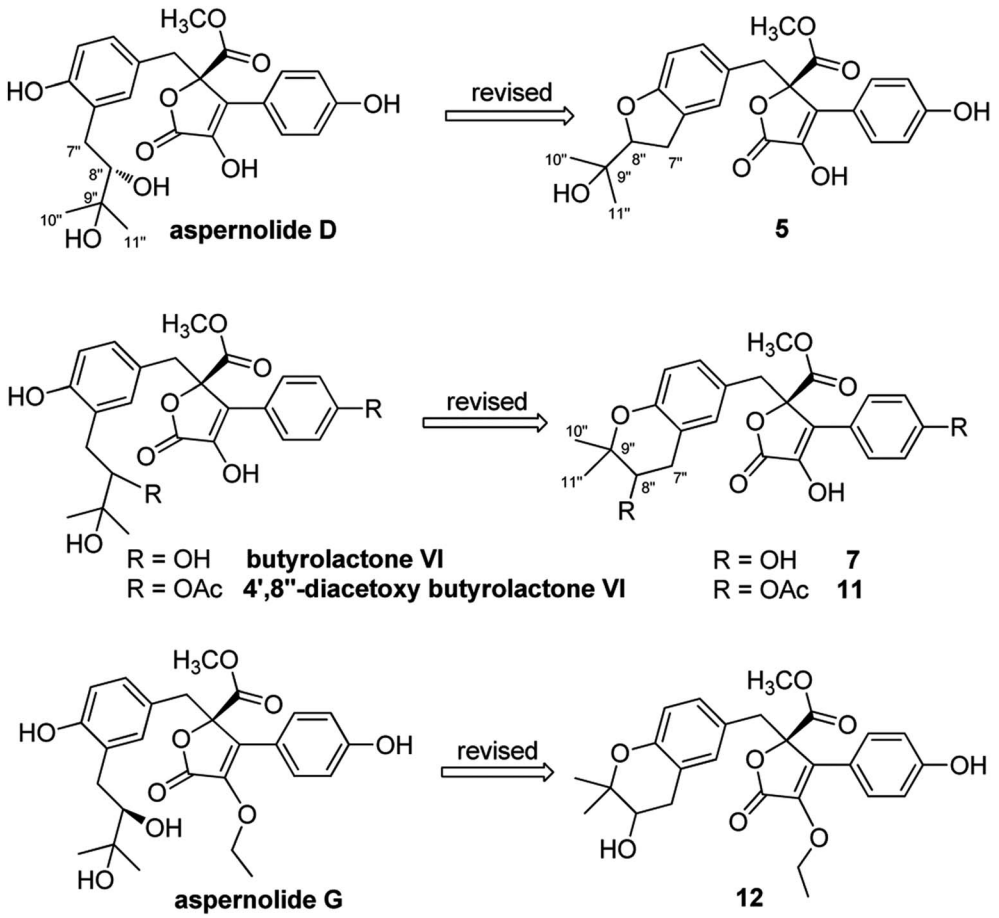

Fig. 5 Structure revisions of aspernolides D and G, butyrolactone VI and 4′,8″-diacetoxy butyrolactone VI.

provide a valuable referenced ^{13}C NMR data (C-7″, C-8″, and C-9″) for structure elucidations of the butenolide derivatives with planar 1-(2-hydroxyphenyl)-3-methylbutane-2,3-diol, 2-(2,3-dihydrobenzofuran-2-yl)propan-2-ol, or 2,2-dimethylchroman-3-ol motifs. However, for the determination of absolute configuration of C-8″, maybe some reliable methods, including

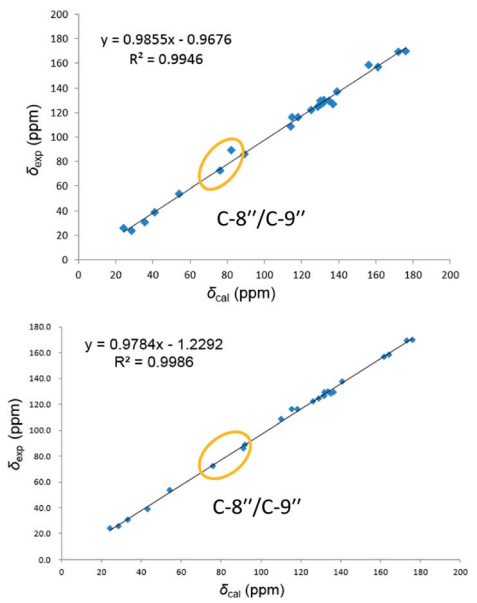

Fig. 6 Linear correlations between the calculated and experimental ^{13}C NMR chemical shifts for aspernolide D (up) and **5** (down).

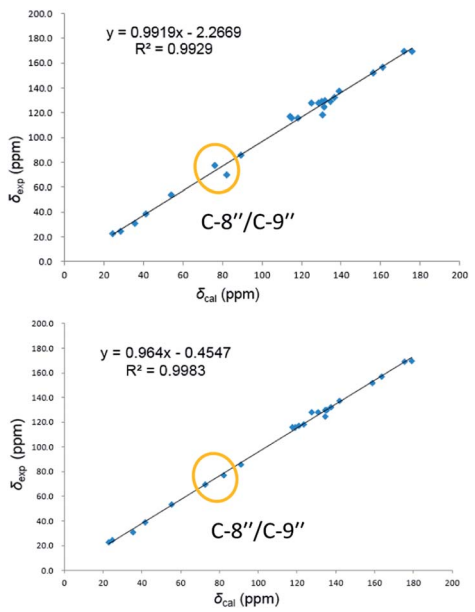

Fig. 7 Linear correlations between the calculated and experimental ^{13}C NMR chemical shifts for butyrolactone VI (up) and **7** (down).

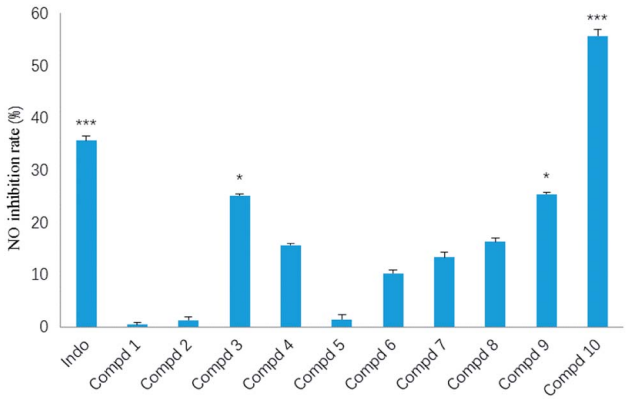

Fig. 8 Inhibitory effect of compounds **1–10** against NO production in LPS-stimulated RAW264.7 cells. The results are expressed as the mean ± SD from three independent experiments. *$p < 0.05$, **$p < 0.01$, ***$p < 0.001$ as compared to LPS group.

Mosher's technique, $[Rh_2(OCOCF_3)_4]$ induced circular dichroism (ICD) spectra, X-ray diffraction crystallography, *etc.*, were best to be used for these compounds.

In our screening of anti-inflammatory agents from natural products,[21] all the isolates (**1–10**) were evaluated for inhibitory effects against NO production in RAW264.7 mouse macrophages induced by lipopolysaccharide (LPS) at a concentration of 20 μM, with indomethacin (50 μM) as the positive control. Among them (Fig. 8), the inhibitory effect of compound **10** (***$p < 0.001$) was even stronger than that of indomethacin. Additionally, compounds **3** and **9** also exerted modest inhibitory effect (*$p < 0.05$) on NO production with inhibition ratios of nearly 25.1% and 25.3%, respectively. The remaining seven compounds (**1**, **2** and **4–8**) were inactive against NO production.

Conclusions

In conclusion, ten butenolide derivatives (**1–10**), including four new ones (**1–4**), were isolated from the coral-derived fungus *Aspergillus terreus*. Remarkably, compounds **1** and **2** were a pair of rare C-8″ epimers with vicinal diol motifs, and the absolute configurations of **1–4** were determined *via* $[Mo_2(AcO)_4]$ induced circular dichroism (ICD) spectra and comparison of their experimental ECD spectra. Importantly, the structures of reported aspernolides D and G, butyrolactone VI and 4′,8″-diacetoxy butyrolactone VI have been correspondingly revised *via* a combined strategy of experimental validations, ^{13}C NMR predictions by ACD/Labs software, and ^{13}C NMR calculations. Remarkably, compounds **3**, **9** and **10** showed remarkable inhibitory effects against NO production, of which compound **10**, was even stronger than that of indomethacin (a positive control), endowing **10** as a promising lead compound for the development of new anti-inflammatory agents. Our findings in this report not only enrich our knowledge about the chemical and pharmacological diversities of butenolide derivatives in the *Aspergillus* genus, but also provide a valuable referenced ^{13}C NMR data (C-7″, C-8″, and C-9″) for structure elucidations of the butenolide derivatives with 1-(2-hydroxyphenyl)-3-methylbutane-2,3-diol, 2-(2,3-dihydrobenzofuran-2-yl)propan-2-ol, or 2,2-dimethylchroman-3-ol motifs.

Experimental section

General experimental procedures

Optical rotations were recorded using a PerkinElmer PE-341 instrument (PerkinElmer, Waltham, MA, USA). UV spectra were recorded with a Varian Cary 50 UV/vis spectrophotometer (Varian, Salt Lake City, UT, USA). IR spectra were measured with a Bruker Vertex 70 FT-IR spectrophotometer (Bruker, Karlsruhe, Germany) with KBr pellets. ECD data were collected with a JASCO-810 spectrometer. 1D and 2D NMR spectra were recorded with a Bruker AM-400 NMR spectrometer (Bruker, Karlsruhe, Germany) using TMS as internal standard. All chemical shifts (δ) were expressed in ppm with reference to the solvent signals for $CDCl_3$ (δ_H 7.24 and δ_C 77.23) or methanol-d_4 (δ_H 3.31 and δ_C 49.0). High-resolution electrospray ionization mass spectrometry (HRESIMS) data were recorded with a Thermo Fisher LTQ XL LC/MS (Thermo Fisher, Palo Alto, CA, USA), by calibrating the instrument with aqueous sodium trifluoroacetate solution and then dissolving and infusing the samples with eluent CH_3CN–H_2O (1 : 1, v/v). Semi-preparative HPLC was performed on an Agilent 1200 liquid chromatograph with Zorbax SB-C_{18} (9.4 mm × 250 mm) column. Silica gel (200–300 mesh, Qingdao Marine Chemical, Inc., Qingdao, People's Republic of China) and Lichroprep RP-C_{18} gel (40–63 μm, Merck, Darmstadt, Germany) were performed for column chromatography (CC). Precoated TLC plates (200–250 μm thickness, silica gel 60 F_{254}, Qingdao Marine Chemical, Inc.) was performed for thin-layer chromatography. Fractions were monitored by TLC and spots were visualized by heating silica gel plates sprayed with 10% H_2SO_4 in EtOH.

Fungus material

The fungal strain *Aspergillus terreus* was isolated from a piece of tissue from the inner part of the soft coral *Sarcophyton subviride* collected from the Xisha Island (16°45′N, 111°65′E) in the South China Sea in October 2016. It was identified by one of the authors (J. Wang) according to its morphology and sequence analysis of the ITS region of the rDNA (GenBank accession no. MF972904). The strain has been deposited in the culture collection of Tongji Medical College, Huazhong University of Science and Technology.

Fermentation, extraction, and isolation

The fungal strain *Aspergillus terreus* was grown on PDA medium at 28 °C for 7 days, which was inoculated statically in 300 × 500 mL Erlenmeyer flasks (each containing 200 g rice and 200 mL water) for 28 days. The whole rice solid medium was extracted seven times in 95% aqueous EtOH at room temperature, and the solvent was concentrated under reduced pressure to afford a total residue, which was then suspended in water and partitioned successfully with EtOAc. The EtOAc extract (1.5 kg) was subjected to silica gel CC eluted with a stepwise gradient of petroleum ether–ethyl acetate–MeOH (10 : 1 : 0, 7 : 1 : 0,

5 : 1 : 0, 3 : 1 : 0, 1 : 1 : 0, 2 : 2 : 1, 1 : 1 : 1) to yield seven fractions (A–G).

Fraction C (75 g) was subjected to an RP-C_{18} column eluted with MeOH–H_2O (from 20 : 80 to 100 : 0, v/v) to afford five fractions (C1–C5). Fraction C3 (2.3 g) was repeatedly separated *via* Sephadex LH-20 eluted with CH_2Cl_2–MeOH (1 : 1, v/v), and followed by silica gel CC (stepwise petroleum ether–ethyl acetate, 4 : 1–1 : 1) and semi-preparative HPLC using MeOH–H_2O (60 : 40, v/v, 2.0 mL min^{-1}), to yield compounds **6** (22.3 mg; t_R 31.5 min), **8** (11.1 mg; t_R 28.2 min) and **9** (36.1 mg; t_R 23.5 min). Fraction C4 (320.5 mg) was purified by semi-preparative HPLC (MeOH–H_2O, 65 : 35, v/v, 3.0 mL min^{-1}) to give compounds **4** (27.6 mg; t_R 28.4 min) and **10** (20.1 mg; t_R 24.6 min).

Fraction D (198 g) was separated by an RP-C_{18} column with MeOH–H_2O (from 20 : 80 to 100 : 0, v/v) as eluent to yield five fractions (D1–D5). Fraction D3 (42 g) was separated through Sephadex LH-20 eluted with CH_2Cl_2–MeOH (1 : 1, v/v) and RP-C_{18} column with MeOH–H_2O (from 20 : 80 to 80 : 20, v/v), and followed by semi-preparative HPLC using CH_3CN–H_2O (60 : 40, v/v, 3.0 mL min^{-1}) to yield compound **3** (13.4 mg; t_R 23.8 min).

Fraction E (186 g) was chromatographed on silica gel CC (CH_2Cl_2–MeOH, 1 : 0–50 : 1, v/v) to yield five main fractions (E1–E5). Fraction E4 (4.6 g) was applied to Sephadex LH-20 using CH_2Cl_2–MeOH (1 : 1, v/v), and followed by semi-preparative HPLC using CH_3CN–H_2O (55 : 45, v/v, 3.0 mL min^{-1}) to afford compounds **5** (19.6 mg; t_R 31.2 min) and **7** (23.2 mg; t_R 34.5 min). Repeated purification of fraction E5 using Sephadex LH-20 with CH_3OH as eluent, RP-C_{18} column (MeOH–H_2O, from 30 : 70 to 100 : 0, v/v), and semi-preparative HPLC (MeOH–H_2O, 62 : 38, v/v, 3.0 mL min^{-1}) afforded compounds **1** (24.0 mg; t_R 25.8 min) and **2** (5.8 mg; t_R 31.5 min).

8″*R*,9″-Diol versicolactone B (1). White, amorphous powder; $[\alpha]_D^{25}$ + 57.0 (*c* 1.00, MeOH); UV (MeOH) λ_{max} (log ε) = 203 (4.62), 286 (4.13), 330 (3.74) nm; ECD (*c* 0.10, MeOH) = $\Delta\varepsilon_{202}$ + 40.44, $\Delta\varepsilon_{230}$ − 9.96, $\Delta\varepsilon_{307}$ + 2.35; IR ν_{max} = 3433, 2976, 1743, 1617, 1501, 1438, 1389, 1259, 1176, 1066, 1041, 798, 763, 695 cm^{-1}; HRESIMS *m*/*z* 481.1255 $[M + K]^+$ (calcd for $C_{24}H_{26}O_8K$, 481.1265); For ^1H NMR and ^{13}C NMR data, see Table 1.

8″*S*,9″-Diol versicolactone B (2). White, amorphous powder; $[\alpha]_D^{25}$ + 92.0 (*c* 1.00, MeOH); UV (MeOH) λ_{max} (log ε) = 203 (4.71), 286 (4.24), 330 (3.82) nm; ECD (*c* 0.10, MeOH) = $\Delta\varepsilon_{201}$ + 44.79, $\Delta\varepsilon_{229}$ − 9.30, $\Delta\varepsilon_{306}$ + 1.95; IR ν_{max} = 3431, 2924, 2851, 1743, 1640, 1546, 1511, 1502, 1440, 1390, 1260, 1180, 1117, 1066, 1041, 764, 694, 563 cm^{-1}; HRESIMS *m*/*z* 465.1529 $[M + Na]^+$ (calcd for $C_{24}H_{26}O_8Na$, 465.1525); For ^1H NMR and ^{13}C NMR data, see Table 1.

3′-Isoamylene butyrolactone IV (3). White, amorphous powder; $[\alpha]_D^{25}$ + 30 (*c* 1.00, MeOH); UV (MeOH) λ_{max} (log ε) = 202 (4.82), 317 (4.28) nm; ECD (*c* 0.17, MeOH) = $\Delta\varepsilon_{206}$ + 18.93, $\Delta\varepsilon_{228}$ − 3.70, $\Delta\varepsilon_{283}$ −6.97; IR ν_{max} = 3437, 2970, 2925, 1746, 1624, 1499, 1443, 1383, 1253, 1175, 1114, 1052 cm^{-1}; HRESIMS *m*/*z* 531.1986 $[M + Na]^+$ (calcd for $C_{29}H_{32}O_8Na$, 531.1995) and *m*/*z* 547.1751 $[M + K]^+$ (calcd for $C_{29}H_{32}O_8K$, 547.1734); For ^1H NMR and ^{13}C NMR data, see Table 1.

4′-Dehydroxy aspernolide A (4). White, amorphous powder; $[\alpha]_D^{25}$ + 67 (*c* 1.00, MeOH); UV (MeOH) λ_{max} (log ε) = 203 (4.64), 221 (4.17), 288 (4.16) nm; ECD (*c* 0.17, MeOH) = $\Delta\varepsilon_{203}$ + 35.21, $\Delta\varepsilon_{227}$ − 12.51, $\Delta\varepsilon_{304}$ + 2.59; IR ν_{max} = 3434, 2973, 2928, 2856, 1743, 1629, 1498, 1260, 1164, 1120, 1039, 764, 608 cm^{-1}; HRESIMS *m*/*z* 431.1464 $[M + Na]^+$ (calcd for $C_{24}H_{24}O_6Na$, 431.1471); For ^1H NMR and ^{13}C NMR data, see Table 1.

$[Mo_2(AcO)_4]$ induced circular dichroism

$[Mo_2(AcO)_4]$ (1 mg) dissolved in DMSO (1 mL) was prepared as the stock solution, to which compounds **1** and **2** (each 0.5 mg) were added, respectively. The circular dichroism (CD) spectra were recorded immediately after mixing and scanned every 10 min for 30 min, to afford the stationary $[Mo_2(AcO)_4]$ induced circular dichroism spectra for each compound.

^{13}C NMR calculations

The conformations generated by BALLOON were subjected to semiempirical PM3 quantum mechanical geometry optimizations using the Gaussian 09 program.[22] Duplicate conformations were identified and removed when the root-mean-square (RMS) distance was less than 0.5 Å for any two geometry-optimized conformations. The remaining conformations were further optimized at the B3LYP/6-31G(d) level in chloroform with the IEFPCM solvation model using Gaussian 09, and the duplicate conformations emerging after these calculations were removed according to the same RMS criteria above. The number of conformers from the conformational search and final optimization for compounds **1**, **5**, and **7** were 400 to 9, 259 to 10, and 160 to 11, respectively. The harmonic vibrational frequencies were calculated to confirm the stability of the final conformers. The NMR chemical shifts were calculated for each conformer at the B3LYP/6-311++G(d,p)//B3LYP/6-31G(d) level with chloroform as solvent by the IEFPCM solvation model implemented in Gaussian 09 program, which were then combined using Boltzmann weighting according to their population contributions.

Anti-inflammatory assay

The anti-inflammatory activity of compounds **1–10** was assessed by measuring the amount of NO production in LPS-induced RAW 264.7 mouse macrophages (positive control, indomethacin), according to the previously described method.[23]

Conflicts of interest

There are no conflicts to declare.

Acknowledgements

We thank the Analytical and Testing Center at HUST for ECD and IR analyses. This project was financially supported by the Program for Changjiang Scholars of Ministry of Education of the People's Republic of China (no. T2016088), the National Science Fund for Distinguished Young Scholars (no. 8172500151), the Innovative Research Groups of the National Natural Science Foundation of China (no. 81721005), the National Natural Science Foundation of China (no. 81573316, 21702067 and 81502943), the China Postdoctoral Science

Foundation Funded Project (no. 2017M610479), the Academic Frontier Youth Team of HUST, and the Integrated Innovative Team for Major Human Diseases Program of Tongji Medical College (HUST).

Notes and references

1 (*a*) M. S. Butler, A. A. B. Robertson and M. A. Cooper, *Nat. Prod. Rep.*, 2014, **31**, 1612–1661; (*b*) E. C. Barnes, R. Kumar and R. A. Davis, *Nat. Prod. Rep.*, 2016, **33**, 372–381; (*c*) A. Schueffler and T. Anke, *Nat. Prod. Rep.*, 2014, **31**, 1425–1448.

2 C. Zhao, H. Liu and W. Zhu, *Acta Microbiol. Sin.*, 2016, **56**, 331–362.

3 H. Zhu, C. Chen, Y. Xue, Q. Tong, X. N. Li, X. Chen, J. Wang, G. Yao, Z. Luo and Y. Zhang, *Angew. Chem., Int. Ed.*, 2015, **54**, 13374–13378.

4 H. Zhu, C. Chen, Q. Tong, X. N. Li, J. Yang, Y. Xue, Z. Luo, J. Wang, G. Yao and Y. Zhang, *Angew. Chem., Int. Ed.*, 2016, **55**, 3486–3490.

5 H. Zhu, C. Chen, Q. Tong, J. Yang, G. Wei, Y. Xue, J. Wang, Z. Luo and Y. Zhang, *Angew. Chem., Int. Ed.*, 2017, **56**, 5242–5246.

6 G. Wei, C. Chen, Q. Tong, J. Huang, W. Wang, Z. Wu, J. Yang, J. Liu, Y. Xue, Z. Luo, J. Wang, H. Zhu and Y. Zhang, *Org. Lett.*, 2017, **19**, 4399–4402.

7 C. Qi, J. Bao, J. Wang, H. Zhu, Y. Xue, X. Wang, H. Li, W. Sun, W. Gao, Y. Lai, J. G. Chen and Y. Zhang, *Chem. Sci.*, 2016, **7**, 6563–6572.

8 Y. He, Z. Hu, W. Sun, Q. Li, X. N. Li, H. Zhu, J. Huang, J. Liu, J. Wang, Y. Xue and Y. Zhang, *J. Org. Chem.*, 2017, **82**, 3125–3131.

9 Z. X. Hu, Y. B. Xue, X. B. Bi, J. W. Zhang, Z. W. Luo, X. N. Li, G. M. Yao, J. P. Wang and Y. H. Zhang, *Mar. Drugs*, 2014, **12**, 5563–5575.

10 P. Nuclear, D. Sommit, N. Boonyuen and K. Pudhom, *Chem. Pharm. Bull.*, 2010, **58**, 1221–1223.

11 A. San-Martin, J. Rovirosa, I. Vaca, K. Vergara, L. Acevedo, D. Vina, F. Orallo and M. C. Chamy, *J. Chil. Chem. Soc.*, 2011, **56**, 625–627.

12 M. Zhou, G. Du, H. Y. Yang, C. F. Xia, J. X. Yang, Y. Q. Ye, X. M. Gao, X. N. Li and Q. F. Hu, *Planta Med.*, 2015, **81**, 235–240.

13 L. D. Bari, G. Pescitelli, C. Pratelli, D. Pini and P. Salvadori, *J. Org. Chem.*, 2001, **66**, 4819–4825.

14 Z. Y. Wu, Y. Wu, G. D. Chen, D. Hu, X. X. Li, X. Sun, L. D. Guo, Y. Li, X. S. Yao and H. Gao, *RSC Adv.*, 2014, **4**, 54144–54148.

15 K. V. Rao, A. K. Sadhukhan, M. Veerender, V. Ravikumar, E. V. S. Mohan, S. D. Dhanvantri, M. Sitaramkumar, J. M. Babu, K. Vyas and G. O. Reddy, *Chem. Pharm. Bull.*, 2000, **48**, 559–562.

16 L. Yuan, W. Huang, K. Zhou, Y. Wang, W. Dong, G. Du, X. Gao, Y. Ma and Q. Hu, *Nat. Prod. Res.*, 2015, **29**, 1914–1919.

17 T. Lin, C. Lu and Y. Shen, *Nat. Prod. Res.*, 2009, **23**, 77–85.

18 F. He, J. Bao, X. Y. Zhang, Z. C. Tu, Y. M. Shi and S. H. Qi, *J. Nat. Prod.*, 2013, **76**, 1182–1186.

19 (*a*) M. W. Lodewyk, M. R. Siebert and D. J. Tantillo, *Chem. Rev.*, 2012, **112**, 1839–1862; (*b*) ACD, Advanced Chemistry Development, Inc., 110 Yonge Street, 14th Floor, Toronto, Ontario, Candada M5C 1T4.

20 S. R. M. Ibrahim, E. S. Elkhayat, G. A. Mohamed, A. I. M. Khedr, M. A. Fouad, M. H. R. Kotb and S. A. Ross, *Phytochem. Lett.*, 2015, **14**, 84–90.

21 Z. Hu, Y. Wu, S. Xie, W. Sun, Y. Guo, X. N. Li, J. Liu, H. Li, J. Wang, Z. Luo, Y. Xue and Y. Zhang, *Org. Lett.*, 2017, **19**, 258–261.

22 (*a*) Z. X. Hu, Y. M. Shi, W. G. Wang, X. N. Li, X. Du, M. Liu, Y. Li, Y. B. Xue, Y. H. Zhang, J. X. Pu and H. D. Sun, *Org. Lett.*, 2015, **17**, 4616–4619; (*b*) Z. X. Hu, Y. M. Shi, W. G. Wang, J. W. Tang, M. Zhou, X. Du, Y. H. Zhang, J. X. Pu and H. D. Sun, *Org. Lett.*, 2016, **18**, 2284–2287.

23 (*a*) Y. J. Li, C. T. Xu, D. D. Lin, J. K. Qin, G. J. Ye and Q. H. Deng, *Bioorg. Med. Chem. Lett.*, 2016, **26**, 3425–3428; (*b*) A. Rajasekaran, V. Sivakumar and S. Darlinquine, *Pharm. Biol.*, 2012, **50**, 1085–1095.